PNAS
www.pnas.org

Supplementary Information for

Ataxin-1 regulates B cell function and the severity of autoimmune experimental encephalomyelitis

Alessandro Didonna[a,1], Ester Canto Puig[a], Qin Ma[a], Atsuko Matsunaga[a], Brenda Ho[a], Stacy J. Caillier[a], Hengameh Shams[a], Nicholas Lee[a], Stephen L. Hauser[a], Qiumin Tan[b], Scott S. Zamvil[a,c], Jorge R. Oksenberg[a]
[a]Weill Institute for Neurosciences, Department of Neurology, University of California, San Francisco, San Francisco, CA 94158
[b]Department of Cell Biology, University of Alberta, Edmonton, Alberta T6G 2H7, Canada
[c]Program in Immunology, University of California, San Francisco, CA 94158

[1]**Corresponding Author:** Alessandro Didonna, Department of Neurology and Weill Institute for Neurosciences, University of California San Francisco, 675 Nelson Rising Lane, San Francisco, CA 94158, USA. **Phone:** +1-415-502-7211; **Email:** alessandro.didonna@ucsf.edu

This PDF file includes:

SI Material and Methods
Figures S1 to S9
Tables S1 to S8
Legends for Datasets S1 to S3

Other supplementary materials for this manuscript include the following:

Datasets S1 to S3

www.pnas.org/cgi/doi/10.1073/pnas.2003798117

SI Materials and Methods

Mouse strains. *Atxn1*$^{-/-}$ mice (B6.129S7-*Atxn1*^{tm2Hzo}/J), *Cic*^{flox} mice (B6(SJL)-*Cic*$^{tm1c(KOMP)Wtsi}$/HzoJ), and *Atxn1l*^{flox} mice (B6;129S7-*Atxn1l*^{tm2Hzo}/J) were a kind gift of Dr. Huda Zoghbi (Baylor College of Medicine, Huston, TX) and have been previously described (1, 2). *CD2-Cre* mice (C57BL/6-Tg(CD2-cre)1Lov/J), *Cd19-Cre* mice (B6.129P2(C)-*Cd19*$^{tm1(cre)Cgn}$/J), *Cd79-Cre* mice (B6.C(Cg)-*Cd79a*$^{tm1(cre)Reth}$/EhobJ), *Sca1*$^{154Q/2Q}$ mice (B6.129S-*Atxn1*^{tm1Hzo}/J), 2D2 mice (C57BL/6-Tg(Tcra2D2,Tcrb2D2)1Kuch/J), and wildtype C57BL/6J mice were purchased from The Jackson Laboratory. Also these transgenic lines were described elsewhere (3-7). All mice were maintained on a pure C57BL/6J background. *Atxn1*$^{-/-}$ and wild type littermates (*Atxn1*$^{+/+}$) were obtained from a heterozygous breeding of *Atxn1*$^{+/-}$ mice. A similar strategy was used to obtain *Sca1*$^{154Q/2Q}$ and *Sca1*$^{2Q/2Q}$ mice as well as *Cre*$^{+/-}$ and *Cre*$^{-/-}$ floxed animals. To avoid possible gender-related confounding affects, only female animals were used for experiments. Mice were housed in a specific pathogen free (SPF) facility and all animal procedures were performed in compliance with experimental guidelines approved by the University of California, San Francisco Committee on Animal Research (CAR).

Antibodies. The following antibodies were used in the study: anti-ATXN1 rabbit polyclonal antibody (8); anti-CIC rabbit polyclonal antibody (NB11059906, Novus Biologicals); anti-β-actin rabbit monoclonal antibody (D6A8, Cell Signaling); anti-GAPDH mouse monoclonal antibody (6C5, Advanced Immunochemical); anti-AKT (pS473) mouse monoclonal antibody (M89-61, BD Biosciences); BTK (pY551)/ ITK (pY511) mouse monoclonal antibody (24a/BTK, BD Biosciences); PLCγ1 (pY783) mouse monoclonal antibody (27/PLC, BD Biosciences); c-CBL (pY700) mouse monoclonal antibody (47/c-Cbl, BD Biosciences); anti-p38 MAPK (pT180/pY182) mouse monoclonal antibody (36/p38, BD Biosciences); anti-ERK1/2 (pT202/pY204) mouse monoclonal antibody (20A, BD Biosciences); anti-STAT1 (pY701) mouse monoclonal antibody (14/P-STAT1, BD Biosciences); anti-STAT3 (pY705) mouse monoclonal antibody (4/P-STAT3, BD Biosciences); anti-STAT4 (pY693) mouse monoclonal antibody (38/p-Stat4, BD Biosciences); anti-STAT5 (pY694) mouse monoclonal antibody (47/Stat5(pY694), BD Biosciences); anti-STAT6 (pY641) mouse monoclonal antibody (18/P-Stat6, BD Biosciences); anti-CD3e hamster monoclonal antibody (145-2C11, BD Biosciences); anti-CD19 rat monoclonal antibody (1D3, BD Biosciences); anti-CD4 rat monoclonal antibody (GK1.5, BD Biosciences); anti-CD8a rat monoclonal antibody (53-6.7, BD Biosciences); anti-CD11b rat monoclonal antibody (B1/70, BD Biosciences); anti-IL-17A rat monoclonal antibody (TC11H10, BD Biosciences); anti-IFNγ rat monoclonal antibody (XMG1.2, BD Biosciences), anti-FOXP3 rat monoclonal antibody (MF23, BD Biosciences); anti-CD44 rat monoclonal antibody (IM7, BD Biosciences); anti-CD80 armenian hamster monoclonal antibody (16-10A1, BioLegend); anti-CD62L rat monoclonal antibody (MEL-14, BD Biosciences); anti-IgD rat monoclonal antibody (11-26c.2a, BD Biosciences); anti-IgM rat monoclonal antibody (R6-60.2, BS Biosciences); anti-CD5 rat monoclonal antibody (53-7.3, BD Biosciences); anti-CD43 rat monoclonal antibody (S7, BD Biosciences); IgG2a κ rat isotype control (R35-95, BD Biosciences); IgG1 κ mouse isotype control (MOPC-21, BD Biosciences).

Active EAE induction. EAE was induced following previously published procedures (9, 10). Briefly, 8-10 week old female mice were injected subcutaneously with 100 µg of MOG_{35-55} peptide (EZBiolab), in complete Freund's adjuvant (CFA) with 4 mg/mL *Mycobacterium tuberculosis* (DIFCO Laboratories). Mice also received 400 ng of pertussis toxin (LIST Biological Laboratories) intraperitoneally both immediately after immunization and 48 hours later. Control mice were injected with everything except the MOG peptide. For all experiments animals were observed daily, and clinical signs were assessed as follows: 0, no signs; 1, decreased tail tone; 2, mild monoparesis or paraparesis; 3, severe paraparesis; 4, paraplegia; 5, quadriparesis; and 6, moribund or death. All scores were assigned blindly to the genotypes of the mice. All animal experiments were conducted according to protocols approved by the local animal welfare committee.

Passive EAE induction. For adoptive transfer experiments, *Atxn1*$^{-/-}$ and *Atxn1*$^{+/+}$ female mice (5-6 per genotype) were primed with 100 µg of MOG_{35-55} in CFA for 10 days. Lymphocytes from

spleens and lymph nodes were then isolated, pooled and cultured *in vitro* for 3 more days in the presence of 10 μg/mL MOG peptide, 20 ng/mL recombinant IL-23 and 10 ng/mL recombinant IL-6. After polarization, either knockout or wildtype cells were injected intraperitoneally into C57BL/6J naïve recipient female mice of 8 weeks of age at the dosage of 10 million cells/mouse. Disease clinical phenotype was assessed daily, following the same scoring system of active EAE experiments.

Western blotting. Mouse cerebella were homogenized in 10 volumes of cold lysis buffer (1% Triton X-100, 50 mM Tris pH 7.5, 75 mM NaCl) supplemented with complete protease inhibitors (Roche). After 10 minutes on ice, lysates were spun at 16,000×g and supernatants collected. B cells were isolated from mouse spleen by positive immunomagnetic selection with Dynabeads (Invitrogen), following a validated protocol which allows at least 95% purity (9). The cells were lysed directly on the beads with Laemmli buffer. All protein samples were separated by SDS-PAGE and then blotted onto nitrocellulose membranes (Immobilion) at 100V for 30 min. Membranes were subsequently blocked with 5% milk in Tris buffered saline with 0.05% Tween-20 (TBS-T) for 1 hour at RT. After blocking, membranes were incubated with primary antibodies diluted (1:1000) in blocking solution ON at 4°C. The day after, the membranes were washed 3 times with TBS-T and incubated with horseradish peroxidase (HRP)-conjugated secondary antibodies (1:5000) in blocking solution for 1 hour at RT. After extensive washing, membranes were incubated with Supersignal West Dura reagent (Thermo Scientific) and the chemiluminescent signals were detected using a Molecular Imager ChemiDoc XRS System equipped with Quantity One software (Bio-Rad).

Cell activation assay. Cell activation was assessed by measuring the surface expression of the activation markers CD44 and CD80 by flow cytometry. In some experiments, splenocytes from naïve *Atxn1*$^{-/-}$ and wildtype female mice were used. In others, mice were first primed with 100 μg of MOG_{35-55} for 10 days and splenocytes were re-stimulated with 1 or 10 μg/mL of MOG peptide for 72 hours in 24-well plates at a concentration of 10^6 cells/mL in complete RPMI 1640 medium. Then, cells in suspension were collected and the adherent cells were detached with PBS-0.05% EDTA on ice for 30 minutes. All cells were then washed with PBS, blocked with Fc blocking reagent (Miltenyi Biotech) and subsequently stained with cell-specific marker antibodies as well as anti-CD44 and anti-CD80 antibodies. Surface expression was finally analyzed using a LSRFortessa instrument equipped with FACSDiva software (BD Biosciences).

Th1, Th17 and Treg differentiation. Untouched $CD4^+$ T cells were isolated by negative immunomagnetic selection using Dynabeads (Invitrogen) from the spleen of naive *Atxn1*$^{-/-}$ and wildtype female mice. Polarization towards the different lineages was promoted with the CytoBox Th1 Kit (Miltenyi Biotech), CellXVivo Mouse Th17 Cell Differentiation Kit and CellXVivo Mouse Treg Cell Differentiation Kit (R&D System), following the manufacturers' instructions. After 72 hours, the percentage of $CD4^+$ T cells differentiated to each cell lineage was quantified by flow cytometry using a LSRFortessa instrument equipped with FACSDiva software (BD Biosciences). Briefly, Th1 and Th17 cells were assessed by intracellular cytokine staining of IFN-γ and IL-17 using the Fixation and Permeabilization Solution Kit (BD Biosciences) after activating the cells for 4 hours with the Cell Activation Cocktail (Fisher) in the presence of Protein Transport Inhibitor Cocktail (Fisher). Treg cell differentiation was instead assessed by FOXP3 staining using the FoxP3 Buffer Set (BD Biosciences).

T-B cell co-cultures. B cells were isolated by positive immunomagnetic selection using anti-CD19 beads (Miltenyi) from *Atxn1*$^{-/-}$ and wildtype female mice either naïve or after 13 days from immunization with 100 μg of MOG peptide in CFA. Untouched $CD4^+$ T cells were isolated by negative immunomagnetic selection using Dynabeads (Invitrogen) from the spleens of 2D2 mice. B cells were treated with 50 μg/mL mitomycin C (Sigma) for 1 hour before being cultured with $CD4^+$ T cells in 96-well plates at a ratio of 5:1 (50,000 B cells and 10,000 T cells per well) in complete RPMI 1640 medium, in the presence of increasing concentrations of MOG peptide. Cells were cultured for 72 hours and pulsed for the last 18 hours with 1 μCi/well [3H]-thymidine before harvesting. Radioactive signals were measured with a 1450 Microbeta Trilux liquid scintillation counter (PerkinElmer).

Phosphoflow cytometry. We have optimized a robust protocol to simultaneously determine by flow cytometry the levels of 7 key signaling phosphoproteins [p38 mitogen-activated protein kinase (p38MAPK), extracellular signal-regulated Kinase 1/2 (ERK1/2) and signal transducers and activators of transcription 1, 3, 4, 5, 6 (STAT1, STAT3, STAT4, STAT5, STAT6)] in three relevant immune cell subsets ($CD4^+$ and $CD8^+$ T cells, and B cells)(11). Briefly, splenocytes were isolated from *Atxn1*$^{-/-}$ and wildtype female mice either naïve or after 10 days from immunization with 100 μg of MOG_{35-55} peptide in CFA. Some cells after priming were re-stimulated in culture with 10 μg/mL of MOG_{35-55} peptide for 24 hours. The splenocytes from the different conditions were fixed with 1.5% PFA and permeabilized with 100% ice-cold methanol for 30 minutes on ice. After washing, cells were stained with fluorophore-conjugated antibodies specific for the different phosphoproteins and cell markers, and analyzed using a LSRFortessa instrument equipped with FACSDiva software (BD Biosciences).

Lymphocyte immunophenotyping. In order to characterize the different lymphocyte sub-populations by flow cytometry, splenocytes were isolated from the spleens of *Atxn1*$^{-/-}$ and wildtype female mice either naïve or after 10 days from immunization with 100 μg of MOG_{35-55} peptide in CFA. All cells were blocked with Fc blocking reagent (Miltenyi Biotech) and subsequently stained with combinations of marker antibodies specific for the different cell subtypes. Within the $CD19^+$ B population, we defined the following cell subtypes: B1a ($CD5^+$, $CD43^+$, IgM^{high}, IgD^{low}); B1b ($CD5^-$, $CD43^+$, IgM^{high}, IgD^{low}); MZ B2 ($CD5^-$, $CD43^-$, IgM^{high}, IgD^{low}); B regulatory ($CD5^+$, $CD43^-$, IgM^{high}, IgD^{low}) and B follicular ($CD5^-$, $CD43^-$, IgM^{low}, IgD^{high}). For $CD4^+$ and $CD8^+$ T cells, we instead defined naïve ($CD44^{low}$,$CD62L^{high}$), central memory ($CD44^{high}$,$CD62L^{high}$), and effector ($CD44^{high}$,$CD62L^{low}$) subtypes. All analyses were conducted using a LSRFortessa instrument equipped with FACSDiva software (BD Biosciences).

Serum immunoglobulin quantification. Total levels of IgG and IgM in the serum of naïve and MOG peptide-primed mice were measured with the Mouse IgG ELISA Kit and Mouse IgM ELISA Kit (Abcam), following manufacturer's instructions. For MOG-specific antibody detection, 96-well plates were coated with 100 μL of MOG_{35-55} (10 μg/mL) in carbonate buffer (BioLegend) overnight at 4° C. The day after, the plates were washed three times with PBS supplemented with 0.05% Tween-20 (PBS-T) and blocked with 3% bovine serum albumin (BSA) in PBS for 1 hour at 37° C. After three washes with PBS-T, serum samples diluted 1:100 in blocking solution were added to the wells and incubated for 2 hours at room temperature (RT). Plates were then washed three more times and HRP-conjugated secondary antibodies diluted 1:2000 in 0.1% BSA in PBS-T were added to the well and incubated for 1 hour at RT. After three final washes, signals were developed using the TBD substrate and detected with a Spectramax plate reader (Molecular Devices).

RNA isolation and RNA-seq. B cells were isolated by positive immunomagnetic selection using anti-CD19 beads (Miltenyi) and total RNA was extracted with the RNeasy Mini Kit (Qiagen). DNA contaminations were removed by on-column digestion using the RNase-free DNase Set (Qiagen). The poly(A) fractions were isolated and converted into sequencing libraries using the mRNA Hyper Prep Kit (KAPA), following the manufacturer's instructions. Next-generation sequencing was performed on a HiSeq X Ten platform (Illumina), generating 30 million of pair-end 150 bp reads per sample. Low-quality and adaptor sequences were trimmed using the Trimmomatic tool. The remaining reads were then aligned to the most recent mouse reference sequence (mm10) using hisat2-2.1.0. The htseq-count tool and Ensembl gtf file were used to count aligned reads for each gene. Differentially expressed genes between genotypes were identified using the edgeR package. P values of 0.05 or less after false discovery rate (FDR) correction were considered significant.

Quantitative RT-PCR analysis. For mRNA analysis, 1μg of total RNA was retro-transcribed into cDNA with the SuperScript III First-Strand kit (Invitrogen), and 0.5 μL of the total reaction volume was used for quantitative RT-PCR. All amplifications were performed on a Mx3005P thermocycler (Stratagene), using the Power SYBR Green PCR Master Mix (Applied Biosystem). Gene expression levels were analyzed using validated primers from the PrimerBank (12) database

(Dataset S3). Each sample was run in triplicate and the $\Delta\Delta C_t$ method was used for relative quantification, with *Gapdh* expression levels serving as internal control.

Histopathology. Mice were perfused with 4% paraformaldehyde (PFA) in phosphate buffered saline (PBS). Spinal cords were dissected and post-fixed in 4% PFA for additional 48 hours before processing for paraffin embedding. Transversal sections of 5 μm were then cut from representative anatomical regions of the spinal cord (cervical, thoracic and lumbar) and stained with hematoxylin and eosin (H&E) for inflammation, with an antibody for myelin basic protein (MBP) for demyelination, and with anti-B220 and anti-CD3 antibodies for infiltrating B and T cells, respectively. Digital images were then acquired and analyzed with a NanoZoomer scanner (Hamamatsu Pothonics). The extent of inflammation was expressed as the number of cell foci (groups of >20 cells) in the spinal cord parenchyma. The level of myelin loss was instead quantified by assigned standard demyelination scores to MBP stains. Finally, B and T cell infiltration was expressed as the area (in pixels) positive to B220 or CD3 antibody stain and normalized to the total area of the spinal cord section. Both tissue processing and histopathological analysis were carried out blindly to the genotypes and were outsourced at Hooke Laboratories (Lawrence, MA).

Bioinformatic analyses. To predict the regulatory effects of the MS-associated variant in the *ATXN1* locus we applied a systems biology approach we have recently developed (13). Briefly, functional data were extracted from RegulomeDB for all the SNPs in linkage with rs719316 ($r^2 \geq 0.5$) and were used to compute weighted scores for each gene in the locus across different cell types, based on the four major cell populations present in the ENCODE and REP databases (B cells, T cells, monocytes and neuronal cells). A gene with a positive score indicates there is evidence that the region containing the MS-associated SNP(s) is actively influencing its transcription in that particular cell type and vice-versa.
The eQTL analysis was performed on the Genotype-Tissue Expression (GTEx) Portal release V8 (14), searching for significant eQTLs of rs719316 in the following tissues: Brain-Cerebellum (n=209), Brain-Cortex (n=205), Spleen (n=227) and Whole Blood (n=670).
Pathway analysis was carried out using Metascape, a web-based portal providing comprehensive gene annotation and enrichment analysis including GO processes, KEGG pathways, and the Reactome gene set (15). The STRING database was instead employed for network analysis (16), selecting only experimentally validated interactions with a high level of confidence (minimum required interaction score=0.700).
To check for enrichment in CIC binding sites, the promoter regions (0.5 kb upstream the TSS) of all DEGs were extracted from the mouse genome assembly mm10 and then used as inputs for the FIMO software (http://meme-suite.org/tools/fimo), looking for exact matches with the CIC consensus motif TGAATG(A/G)A on both DNA strands. Statistical significance was tested by calculating the frequency distribution of CIC motifs identified in pools of genes of the same size of each DEG list, randomly sampled from the mouse genome 1000 times.

Statistical analyses. Differences between means of two groups were assessed with two-tailed Student's t-test. Differences in cell infiltration were assessed by one-tailed Student's t-test. Differences in mortality rates were assessed by Fisher's exact test. P values equal to 0.05 or less were considered significant. Data were expressed as mean ±SEM. All statistical analyses were computed using GraphPad Prism 8.3.1 or code written in R software (r-project.org) 3.3.1 version. To generate heatmaps, the mean fluorescence intensity (MFI) values (of protein phosphorylation or surface expression) for each protein in each cell type were first transformed into Z-scores and then averaged across each genotype. Mean Z-scores were plotted according to the following color code: proteins displaying values higher than the mean are depicted in red while proteins shown values lower than the mean are depicted in blue. Proteins showing values equal to the mean are instead represented in white.

References

1. Matilla A*, et al.* (1998) Mice lacking ataxin-1 display learning deficits and decreased hippocampal paired-pulse facilitation. *J Neurosci* 18(14):5508-5516.
2. Lu HC*, et al.* (2017) Disruption of the ATXN1-CIC complex causes a spectrum of neurobehavioral phenotypes in mice and humans. *Nat Genet* 49(4):527-536.
3. Vacchio MS*, et al.* (2014) A ThPOK-LRF transcriptional node maintains the integrity and effector potential of post-thymic CD4+ T cells. *Nat Immunol* 15(10):947-956.
4. Hobeika E*, et al.* (2006) Testing gene function early in the B cell lineage in mb1-cre mice. *Proc Natl Acad Sci USA* 103(37):13789-13794.
5. Watase K*, et al.* (2002) A long CAG repeat in the mouse Sca1 locus replicates SCA1 features and reveals the impact of protein solubility on selective neurodegeneration. *Neuron* 34(6):905-919.
6. Rickert RC, Roes J, & Rajewsky K (1997) B lymphocyte-specific, Cre-mediated mutagenesis in mice. *Nucleic Acids Res* 25(6):1317-1318.
7. Bettelli E*, et al.* (2003) Myelin oligodendrocyte glycoprotein-specific T cell receptor transgenic mice develop spontaneous autoimmune optic neuritis. *J Exp Med* 197(9):1073-1081.
8. Burright EN*, et al.* (1995) SCA1 transgenic mice: a model for neurodegeneration caused by an expanded CAG trinucleotide repeat. *Cell* 82(6):937-948.
9. Didonna A, Cekanaviciute E, Oksenberg JR, & Baranzini SE (2016) Immune cell-specific transcriptional profiling highlights distinct molecular pathways controlled by Tob1 upon experimental autoimmune encephalomyelitis. *Sci Rep* 6:31603.
10. Didonna A*, et al.* (2019) Sex-specific Tau methylation patterns and synaptic transcriptional alterations are associated with neural vulnerability during chronic neuroinflammation. *J Autoimmun* 101:56-69.
11. Canto E*, et al.* (2018) Aberrant STAT phosphorylation signaling in peripheral blood mononuclear cells from multiple sclerosis patients. *J Neuroinflammation* 15(1):72.
12. Spandidos A, Wang X, Wang H, & Seed B (2010) PrimerBank: a resource of human and mouse PCR primer pairs for gene expression detection and quantification. *Nucleic Acids Res* 38(Database issue):D792-799.
13. International Multiple Sclerosis Genetics Consortium (2019) A systems biology approach uncovers cell-specific gene regulatory effects of genetic associations in multiple sclerosis. *Nat Commun* 10(1):2236.
14. GTEx Consortium (2013) The Genotype-Tissue Expression (GTEx) project. *Nat Genet* 45(6):580-585.
15. Zhou Y*, et al.* (2019) Metascape provides a biologist-oriented resource for the analysis of systems-level datasets. *Nat Commun* 10(1):1523.
16. Szklarczyk D*, et al.* (2019) STRING v11: protein-protein association networks with increased coverage, supporting functional discovery in genome-wide experimental datasets. *Nucleic Acids Res* 47(D1):D607-D613.

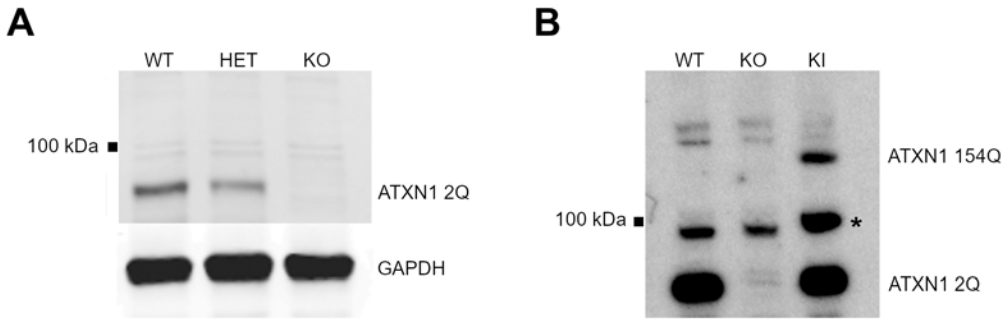

Figure S1. Ataxin-1 expression in *Atxn1* knockout and knock-in mice. (**A**) Cerebellar lysates from *Atxn1*$^{+/+}$ (WT), *Atxn1*$^{+/-}$ (HET) and *Atxn1*$^{-/-}$ (KO) animals were probed for ataxin-1 levels by Western blotting using a polyclonal antibody. Glyceraldehyde-3-Phosphate Dehydrogenase (GAPDH) levels were used as loading control. *Atxn1*-null mice did not show any band at expected ataxin-1 molecular weight (~95 kDa), while wildtype mice displayed a signal whose intensity was roughly double the one from heterozygous animals. (**B**) The same polyclonal antibody was used to confirm the expression of mutant ataxin-1 in cerebellar lysates from *Atxn1*$^{154Q/2Q}$ mice (KI). *Atxn1*$^{+/+}$ (WT) and *Atxn1*$^{-/-}$ (KO) mice were used as positive and negative controls, respectively. Both wildtype and knock-in animals showed a signal corresponding to endogenous ataxin-1 bearing 2 glutamines (ATXN1 2Q) while only knock-in mice displayed an additional band compatible with mutant ataxin-1 bearing 154 glutamines (ATXN1 154Q). Conversely, *Atxn1*-null samples lacked those signals. A non-specific signal (asterisk) was also detected in all samples at 100 kDa.

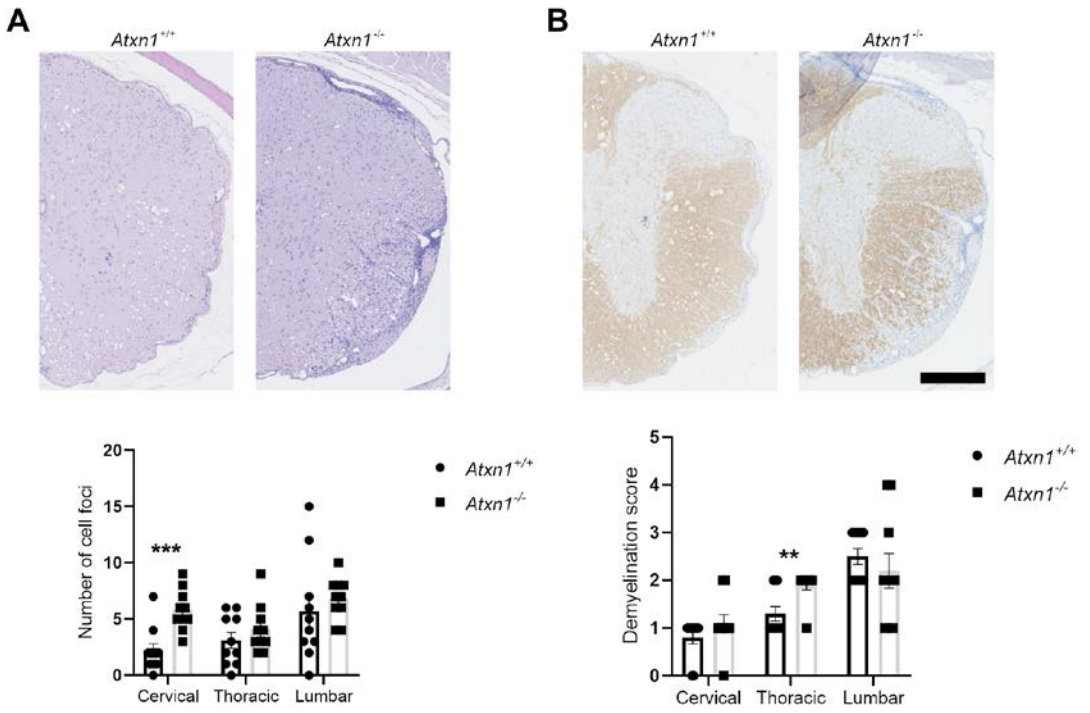

Figure S2. Histological analysis of spinal cords from *Atxn1*$^{-/-}$ and wildtype mice upon EAE. (**A**) Paraffin-embedded sections from spinal cords (cervical, thoracic and lumbar regions) were collected at 30 dpi of passive EAE and stained with hematoxylin and eosin (H&E). Inflammation was measured as the number of cell foci (groups of >20 infiltrating immune cells) in representative sections of each spinal cord region. A significant increase in infiltrating immune cells was quantified in the cervical region of *Atxn1*$^{-/-}$ mice (n=10 mice per group). (**B**) Representative sections were also stained for myelin basic protein (MBP) and myelin loss was assessed in the different spinal cord regions. Significantly higher demyelination scores were assigned the thoracic cervical of *Atxn1*$^{-/-}$ mice (n=10 mice per group). Scale bar: 250 μm. Differences between groups were assessed by two-tailed Student's t-test. **P≤0.01, ***P≤0.001.

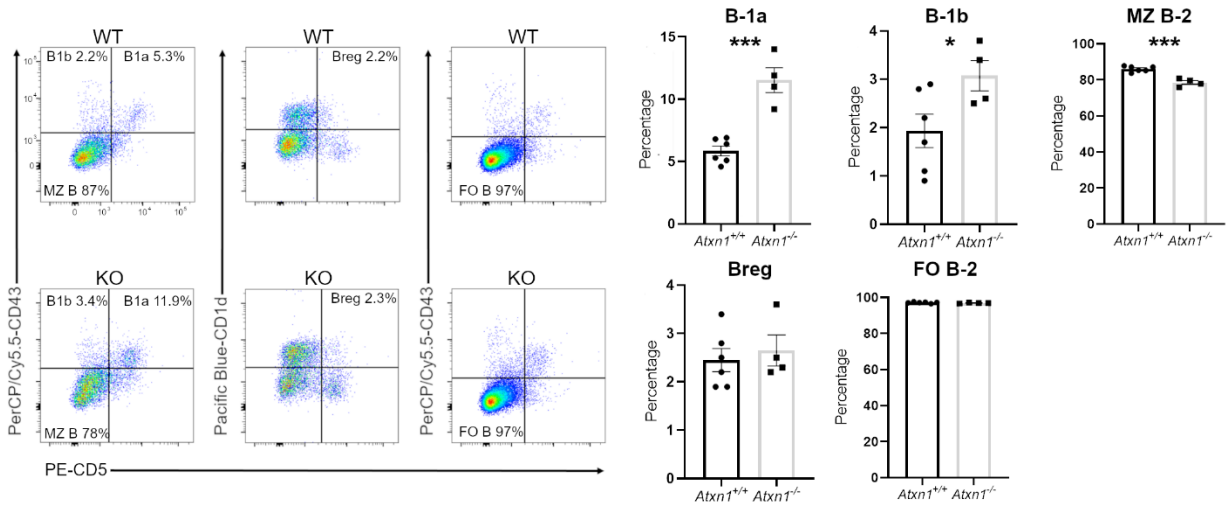

Figure S3. Immunophenotyping of B cells from MOG peptide immunized mice. Splenocytes from *Atxn1*$^{-/-}$ and wildtype mice at day 10 post-immunization with 100 μg MOG peptide were analyzed by flow cytometry to measure the percentage of different CD19^{+} B cell sub-populations. A significant increase was measured for B-1a (CD5^{+},CD43^{+},IgM^{hi},IgD^{low}) and B-1b (CD5^{-},CD43^{+},IgM^{high},IgD^{low}) subsets in knockout animals as compared to controls, while marginal zone B-2 cells (CD5^{-},CD43^{-},IgM^{high},IgD^{low}) were significantly decreased. No differences were instead measured in the percentage of regulatory (CD5^{+},CD43^{-},IgM^{high},IgD^{low}) and follicular B-2 (CD5^{-},CD43^{-},IgM^{low},IgD^{high}) B cell populations between the two genotypes (n=4-6 mice per group). Differences between groups were assessed by two-tailed Student's t-test. *P≤0.05, ***P≤0.001.

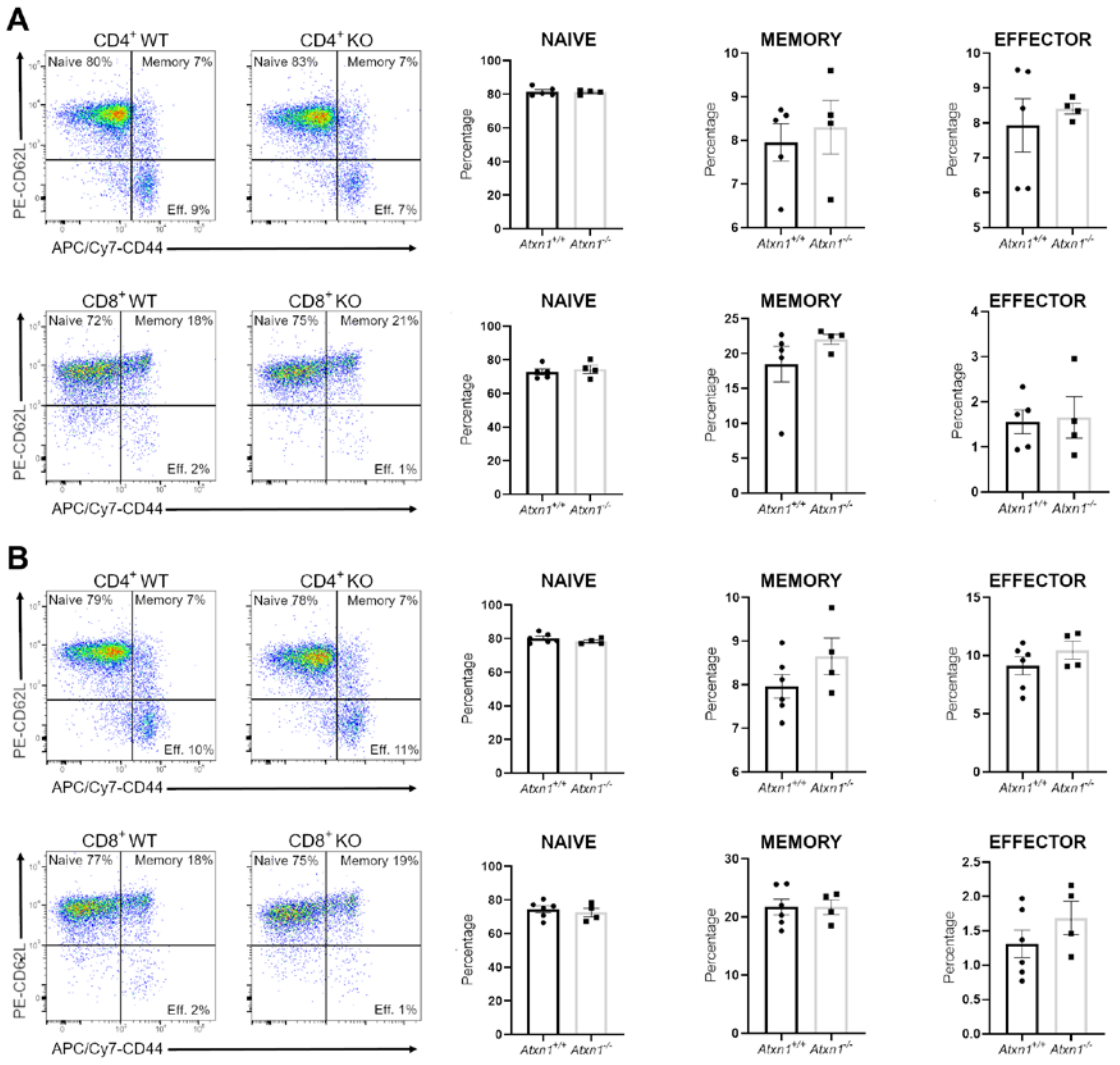

Figure S4. Immunophenotyping of T cells. (**A**) Splenocytes from *Atxn1*$^{-/-}$ and wildtype mice were analyzed by flow cytometry for different CD4^{+} T cell sub-populations. No differences were measured in the percentage of naïve (CD44^{low},CD62L^{high}), central memory (CD44^{high},CD62L^{high}), and effector (CD44^{high},CD62L^{low}) subsets. The same populations were also analyzed in CD8^{+} T cells and also in this case no differences were found in the percentages of naïve, central memory and effector subsets (n=4-5 mice per group). (**B**) Immunophenotyping of CD4^{+} T cell sub-populations from *Atxn1*$^{-/-}$ and wildtype mice at day 10 post-immunization with 100 μg MOG peptide. For either CD4^{+} and CD8^{+} T cells, no differences were measured in the percentage of naïve (CD44^{low},CD62L^{high}), central memory (CD44^{high},CD62L^{high}), and effector (CD44^{high},CD62L^{low}) subsets (n=4-6 mice per group). Differences between groups were assessed by two-tailed Student's t-test.

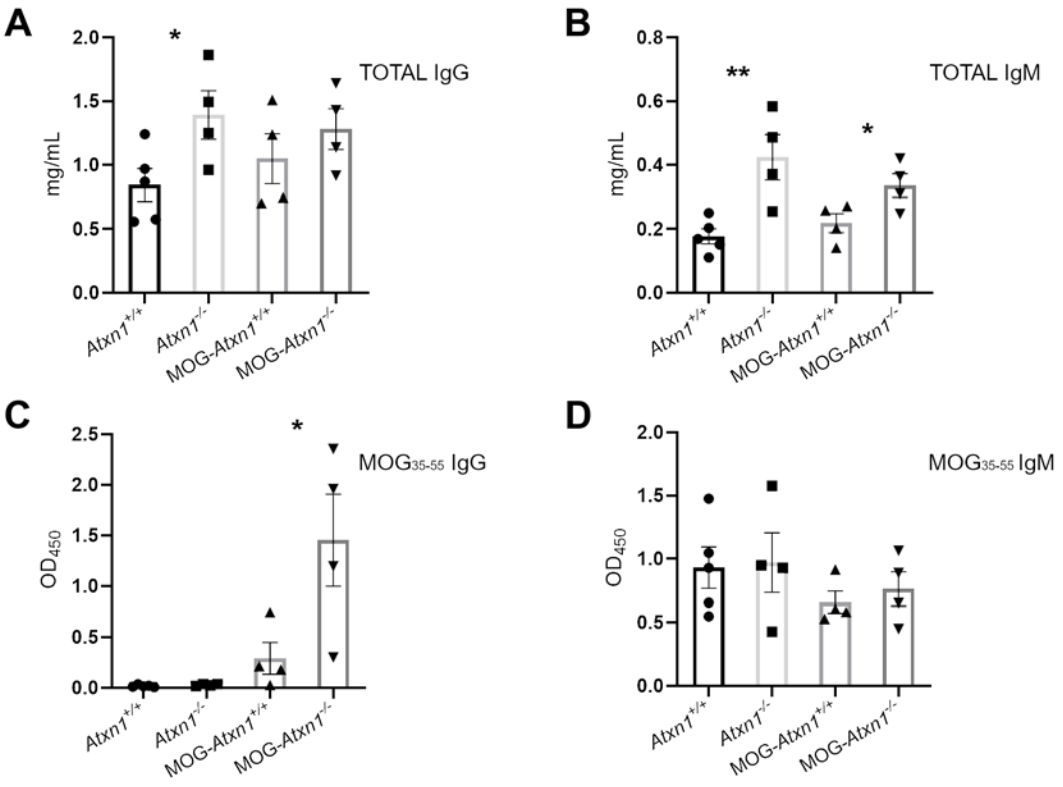

Figure S5. Analysis of humoral response. (**A**, **B**) Total levels of immunoglobulins (IgG and IgM) were measured by ELISA in serum of mice, either naïve or 10 days after priming with 100 μg MOG peptide in CFA. Increased levels of both IgG and IgM were found in naïve *Atxn1*$^{-/-}$ animals as compared to wildtype controls. Higher levels of IgM persisted also after MOG peptide immunization (n=4 mice per group). (**C**, **D**) Immunoglobulins toward MOG peptide were also measured by ELISA. Increased anti-MOG-specific IgG levels but not IgM were measured in primed *Atxn1*$^{-/-}$ mice (n=4 mice per group). Differences between groups were assessed by two-tailed Student's t-test. *P≤0.05, **P≤0.01.

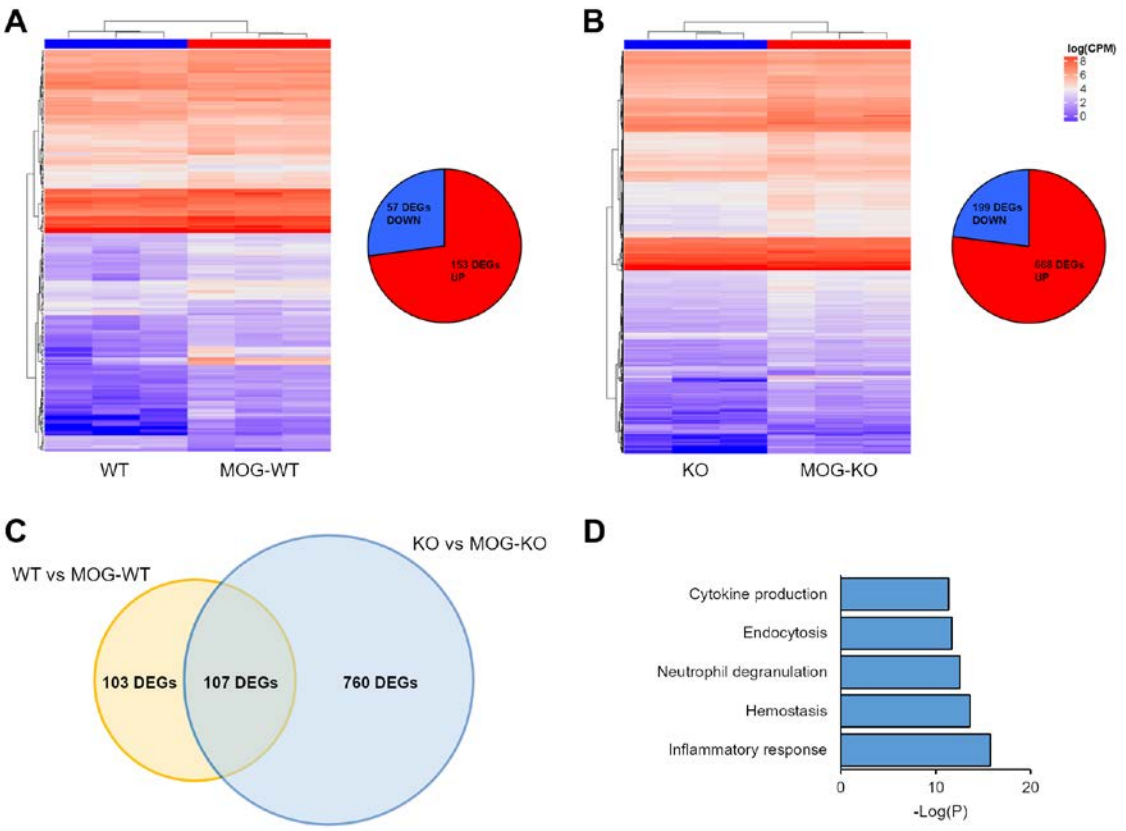

Figure S6. Longitudinal analysis of gene expression in B cells from *Atxn1*$^{-/-}$ and wildtype mice. (**A**, **B**) Unsupervised hierarchical clustering of logCPM values of the differentially expressed genes (DEGs) in B cells from wildtype and *Atxn1*$^{-/-}$ mice at baseline and after MOG peptide immunization (n=3 mice per group). (**C**) Venn diagrams showing the overlap of DEGs between wildtype and *Atxn1*$^{-/-}$ B cells. (**D**) Histograms showing the top 5 most significant gene ontology (GO) terms in the biological process category for the *Atxn1*$^{-/-}$ specific DEGs.

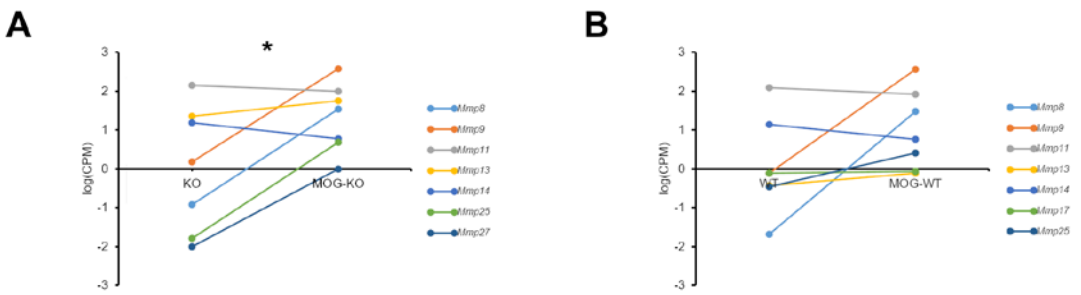

Figure S7. Genes encoding matrix metalloproteinases are upregulated in B cells from *Atxn1*$^{-/-}$ mice. (**A**) Trajectories of the matrix metalloproteinase genes (*Mmp8*, *Mmp9*, *Mmp11*, *Mmp13*, *Mmp14*, *Mmp25*, *Mmp27*) expressed in knockout B cells at baseline and upon MOG peptide stimulation. (**B**) Trajectories of all the matrix metalloproteinase genes (*Mmp8*, *Mmp9*, *Mmp11*, *Mmp13*, *Mmp14*, *Mmp17*, *Mmp25*) expressed in wildtype B cells at the same time points. Log2(CPM) values from the RNA-seq datasets were used to plot the graphs. Differences between groups were assessed by two-tailed Student's t-test. *P≤0.05.

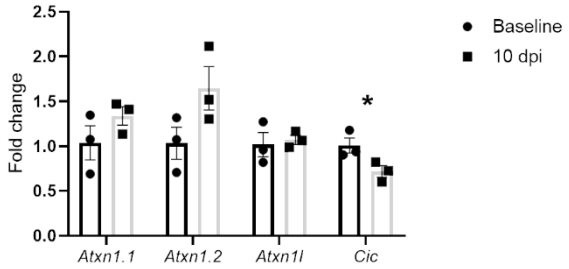

Figure S8. Expression analysis of ataxin-1 interactors in B cells. The levels of *Atxn1* (both isoforms), *Atxn1l* and *Cic* transcripts were measured by qRT-PCR in B cells isolated from wildtype naïve (black bars) and MOG peptide immunized mice (10 dpi, grey bars). *Cic* expression was significantly decreased upon MOG peptide challenge. A trend for higher levels of *Atxn1* isoforms was detected in B cells after MOG peptide immunization, while no differences were detected for *Atxn1l*. Differences between groups were assessed by two-tailed Student's t-test. *P≤0.05.

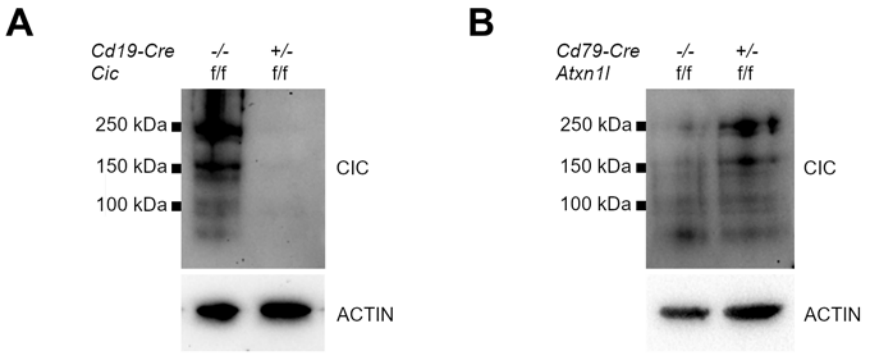

Figure S9. Capicua (CIC) expression in B cell conditional *Cic* and *Atxn1l* knockout mice. (**A**) B cell lysates from CIC-null animals (*Cd19-Cre*$^{+/-}$;*Cic*$^{flox/flox}$) and controls (*Cd19-Cre*$^{-/-}$;*Cic*$^{flox/flox}$) were probed for CIC levels by Western blotting with a polyclonal antibody. Actin levels served as loading controls. Controls showed a signal compatible with CIC (>200 kDa) while CIC-null mice did not show any signal at the same molecular weight. (**B**) CIC levels were also tested in B cells lysates from ATXN1L-null mice (*Cd79-Cre*$^{+/-}$;*Atxn1l*$^{flox/flox}$) and controls (*Cd79-Cre*$^{-/-}$;*Atxn1l*$^{flox/flox}$). The same band pattern was found in both genotypes, suggesting that ATXN1L ablation does not destabilize CIC. Pools of 3 mice per genotype were used in all analyses.

		BASELINE		MOG_{35-55} (1 μg/mL)		MOG_{35-55} (10 μg/mL)	
Cell type	**Group**	**CD80**	**CD44**	**CD80**	**CD44**	**CD80**	**CD44**
$CD4^+$ T cells	WT	0.001 (0.333)	0.402 (0.212)	-0.086 (0.264)	0.276 (0.417)	0.106 (0.316)	0.248 (0.313)
	KO	-0.001 (0.265)	-0.402 (0.323)	0.086 (0.421)	-0.276 (0.232)	-0.106 (0.382)	-0.248 (0.366)
	P-value	0.995	**0.052**	0.734	0.272	0.673	0.321
$CD8^+$ T cells	WT	0.268 (0.298)	0.521 (0.300)	0.465 (0.321)	0.199 (0.359)	-0.005 (0.269)	0.027 (0.314)
	KO	-0.268 (0.279)	-0.521 (0.192)	-0.465 (0.290)	-0.199 (0.330)	0.005 (0.421)	-0.027 (0.388)
	P-value	0.204	**0.009**	**0.049**	0.426	0.983	0.914
B cells	WT	-0.646 (0.253)	-0.570 (0.209)	-0.565 (0.187)	-0.055 (0.296)	-0.709 (0.071)	-0.361 (0.332)
	KO	0.646 (0.184)	0.570 (0.269)	0.565 (0.351)	0.055 (0.401)	0.709 (0.317)	0.361 (0.319)
	P-value	**$6.14x10^{-4}$**	**0.003**	**0.016**	0.828	**0.002**	0.138
Monocytes	WT	-0.109 (0.267)	0.193 (0.280)	-0.506 (0.149)	0.004 (0.275)	-0.470 (0.231)	0.368 (0.329)
	KO	0.109 (0.328)	-0.193 (0.309)	0.506 (0.392)	-0.004 (0.416)	0.470 (0.365)	-0.368 (0.320)
	P-value	0.610	0.364	**0.039**	0.985	**0.050**	0.130

Table S1. Z-scores (mean ± SE) of CD80 and CD44 surface levels between *Atxn1*-null and wildtype mice (n=11) before after *in vitro* stimulation with crescent concentrations of MOG peptide. Differences between groups were assessed by two-tailed Student's t-test.

Gene	WT (FC ± SE)	KO (FC ± SE)	P-value
Robo1	1.00 ± 0.09	6.07 ± 0.71	0.002
Ctla4	1.06 ± 0.24	3.19 ± 0.55	0.024
Lag3	1.00 ± 0.04	0.49 ± 0.02	0.0008
Pla2g2d	1.00 ± 0.08	0.33 ± 0.03	0.002
Ntng2	1.05 ± 0.22	2.35 ± 0.17	0.010
H1f0	1.02 ± 0.17	1.72 ± 0.16	0.042
Emb	1.00 ± 0.08	1.97 ± 0.20	0.011
Gpr55	1.03 ± 0.18	2.25 ± 0.25	0.018
Bhlhe41	1.02 ± 0.15	2.20 ± 0.23	0.013
Nid1	1.00 ± 0.08	1.97 ± 0.15	0.005
Mfhas1	1.01 ± 0.11	1.43 ± 0.11	0.058
Bcl6	1.00 ± 0.01	0.81 ± 0.04	0.017
Fcrl5	1.00 ± 0.08	1.71 ± 0.21	0.037
Cd36	1.00 ± 0.07	1.55 ± 0.19	0.057

Table S2. qRT-PCR validation of candidate genes from GO category “regulation of cell activation” that are differentially expressed between *Atxn1*-null and wildtype B cells (n=3) in baseline conditions. Differences between groups were assessed by two-tailed Student’s t-test.

Gene	MOG-WT (FC ± SE)	MOG-KO (FC ± SE)	P-value
Cdk14	1.00 ± 0.05	1.48 ± 0.13	0.031
Rara	1.00 ± 0.04	0.69 ± 0.04	0.007
Eya1	1.02 ± 0.16	0.48 ± 0.03	0.035
Spag5	1.02 ± 0.16	1.62 ± 0.13	0.050
Tnf	1.00 ± 0.03	0.60 ± 0.02	0.001
Ube2c	1.01 ± 0.13	1.57 ± 0.13	0.044
Pbx1	1.00 ± 0.05	0.47 ± 0.04	0.001
Prkcq	1.00 ± 0.09	0.64 ± 0.08	0.044
Cd300lf	1.00 ± 0.06	1.76 ± 0.11	0.004
Thy1	1.01 ± 0.12	0.56 ± 0.05	0.027
Rad54l	1.01 ± 0.12	1.66 ± 0.07	0.010
Cenph	1.00 ± 0.06	1.54 ± 0.08	0.007
Birc5	1.02 ± 0.15	1.51 ± 0.10	0.057
Lats2	1.00 ± 0.04	0.67 ± 0.03	0.005
Mylip	1.00 ± 0.02	0.67 ± 0.04	0.003
Sgk1	1.00 ± 0.01	0.54 ± 0.04	0.001
Dnajb1	1.00 ± 0.03	0.54 ± 0.02	0.0006
Gpr55	1.00 ± 0.06	2.31 ± 0.17	0.002
Ctla4	1.00 ± 0.06	1.83 ± 0.28	0.047
Prc1	1.01 ± 0.12	1.41 ± 0.09	0.059
Cdkn1b	1.00 ± 0.02	0.58 ± 0.04	0.001

Table S3. qRT-PCR validation of candidate genes from GO category “mitotic cell cycle progress” that are differentially expressed between Atxn1-null and wildtype B cells (n=3) isolated from MOG peptide injected mice (10 dpi). Differences between groups were assessed by two-tailed Student’s t-test.

Gene	KO (FC ± SE)	MOG-KO (FC ± SE)	P-value
Axl	1.00 ± 0.05	1.54 ± 0.12	0.017
Tgm2	1.01 ± 0.13	2.07 ± 0.33	0.043
Treml4	1.00 ± 0.04	1.70 ± 0.17	0.016
C1qa	1.01 ± 0.11	1.63 ± 0.16	0.036
C1qb	1.03 ± 0.18	2.64 ± 0.25	0.007
C1qc	1.01 ± 0.14	1.86 ± 0.29	0.059
Cd5l	1.00 ± 0.04	2.06 ± 0.35	0.040
Slc11a1	1.00 ± 0.08	1.84 ± 0.16	0.011
Anxa2	1.00 ± 0.03	1.31 ± 0.06	0.013
Igf1	1.00 ± 0.04	1.74 ± 0.18	0.016
Tnfrsf1a	1.00 ± 0.05	1.56 ± 0.13	0.019
Gas6	1.03 ± 0.18	9.09 ± 1.55	0.006
Ada	1.00 ± 0.03	1.45 ± 0.16	0.055
C6	1.00 ± 0.08	1.54 ± 0.14	0.036
Tlr8	1.01 ± 0.12	1.87 ± 0.29	0.054
Il18	1.00 ± 0.04	1.48 ± 0.11	0.018
Cd59a	1.00 ± 0.08	1.66 ± 0.11	0.010

Table S4. qRT-PCR validation of candidate genes from GO category “inflammation response” that are differentially expressed in B cells isolated from Atxn1-null mice (n=3) before and after MOG peptide immunization (10 dpi). Differences between groups were assessed by two-tailed Student’s t-test.

Gene	WT (FC ± SE)	MOG-WT (FC ± SE)	P-value
Axl	1.00 ± 0.09	1.43 ± 0.18	0.108
Tgm2	1.01 ± 0.10	1.38 ± 0.15	0.115
Treml4	1.00 ± 0.05	1.23 ± 0.10	0.121
C1qa	1.01 ± 0.07	1.44 ± 0.27	0.198
C1qb	1.07 ± 0.24	1.26 ± 0.33	0.664
C1qc	1.00 ± 0.05	1.69 ± 0.32	0.104
Cd5l	1.01 ± 0.11	1.26 ± 0.23	0.378
Slc11a1	1.02 ± 0.13	1.49 ± 0.17	0.101
Anxa2	1.00 ± 0.09	1.24 ± 0.22	0.396
Igf1	1.04 ± 0.20	1.57 ± 0.39	0.295
Tnfrsf1a	1.00 ± 0.10	1.53 ± 0.19	0.074
Gas6	1.28 ± 0.56	3.69 ± 0.99	0.102
Ada	1.01 ± 0.10	1.21 ± 0.26	0.516
C6	1.02 ± 0.16	1.53 ± 0.23	0.150
Tlr8	1.01 ± 0.11	1.38 ± 0.12	0.097
Il18	1.00 ± 0.06	1.02 ± 0.14	0.917
Cd59a	1.08 ± 0.29	1.63 ± 0.31	0.277

Table S5. qRT-PCR validation of candidate genes from GO category “inflammation response” that are not differentially expressed in B cells isolated from wildtype mice (n=3) before and after MOG peptide immunization (10 dpi). Differences between groups were assessed by two-tailed Student’s t-test.

Cell type	Group	p38MAPK	ERK1/2	STAT1	STAT3	STAT4	STAT5	STAT6
B cells	WT	-0.522 (0.256)	-0.289 (0.216)	-0.007 (0.257)	-0.298 (0.301)	-0.163 (0.273)	-0.007 (0.279)	-0.328 (0.295)
	KO	0.522 (0.247)	0.289 (0.343)	0.007 (0.340)	0.298 (0.270)	0.163 (0.319)	0.007 (0.321)	0.328 (0.269)
	P-value	**0.008**	0.172	0.973	0.156	0.445	0.970	0.116
$CD4^+$ T cells	WT	-0.262 (0.267)	-0.281 (0.222)	0.115 (0.303)	-0.283 (0.246)	-0.136 (0.291)	0.147 (0.345)	-0.134 (0.294)
	KO	0.262 (0.310)	0.281 (0.341)	-0.115 (0.295)	0.283 (0.323)	0.136 (0.304)	-0.147 (0.240)	0.134 (0.302)
	P-value	0.215	0.185	0.592	0.180	0.524	0.493	0.530
$CD8^+$ T cells	WT	-0.133 (0.268)	-0.242 (0.220)	0.153 (0.257)	-0.034 (0.253)	0.155 (0.234)	0.255 (0.308)	-0.044 (0.241)
	KO	0.133 (0.325)	0.242 (0.348)	-0.153 (0.332)	0.034 (0.342)	-0.155 (0.349)	-0.255 (0.271)	0.044 (0.351)
	P-value	0.534	0.255	0.475	0.873	0.468	0.228	0.835

Table S6. Z-scores (mean ± SE) of phosphorylated protein levels in different immune cell populations isolated from *Atxn1*-null and wildtype mice (n=11) in baseline conditions. Differences between groups were assessed by two-tailed Student's t-test.

Cell type	Group	p38MAPK	ERK1/2	STAT1	STAT3	STAT4	STAT5	STAT6
B cells	WT	-0.446 (0.229)	-0.603 (0.219)	-0.736 (0.218)	0.057 (0.405)	-0.022 (0.341)	-0.154 (0.376)	-0.134 (0.331)
	KO	0.446 (0.374)	0.603 (0.312)	0.736 (0.217)	-0.057 (0.291)	0.022 (0.364)	0.154 (0.318)	0.134 (0.367)
	P-value	0.065	**0.007**	**2.93×10^{-4}**	0.822	0.928	0.542	0.595
$CD4^+$ T cells	WT	-0.604 (0.155)	-0.658 (0.222)	-0.743 (0.227)	-0.482 (0.318)	-0.050 (0.330)	-0.413 (0.336)	-0.160 (0.330)
	KO	0.604 (0.348)	0.658 (0.277)	0.743 (0.200)	0.482 (0.285)	0.050 (0.374)	0.413 (0.295)	0.160 (0.365)
	P-value	**0.010**	**0.002**	**2.44×10^{-4}**	**0.040**	0.841	0.086	0.524
$CD8^+$ T cells	WT	-0.514 (0.118)	-0.566 (0.206)	-0.729 (0.213)	-0.310 (0.326)	0.182 (0.349)	-0.293 (0.280)	-0.528 (0.208)
	KO	0.514 (0.400)	0.566 (0.340)	0.729 (0.229)	0.310 (0.340)	-0.182 (0.344)	0.293 (0.383)	0.528 (0.355)
	P-value	**0.038**	**0.015**	**3.75×10^{-4}**	0.209	0.467	0.238	**0.025**

Table S7. Z-scores (mean ± SE) of phosphorylated protein levels in different immune cell populations isolated from *Atxn1*-null and wildtype mice (n=8) after MOG peptide priming for 10 days. Differences between groups were assessed by two-tailed Student's t-test.

Cell type	Group	p38MAPK	ERK1/2	STAT1	STAT3	STAT4	STAT5	STAT6
B cells	WT	-0.089 (0.323)	-0.425 (0.309)	-0.637 (0.188)	0.013 (0.369)	0.350 (0.345)	-0.025 (0.362)	0.045 (0.353)
	KO	0.089 (0.378)	0.425 (0.320)	0.637 (0.313)	-0.013 (0.336)	-0.350 (0.308)	0.025 (0.344)	-0.045 (0.352)
	P-value	0.725	0.077	**0.004**	0.956	0.153	0.921	0.858
$CD4^+$ T cells	WT	-0.408 (0.327)	-0.525 (0.271)	-0.535 (0.203)	-0.643 (0.235)	0.047 (0.306)	-0.311 (0.364)	-0.045 (0.372)
	KO	0.408 (0.307)	0.525 (0.312)	0.535 (0.356)	0.643 (0.275)	-0.047 (0.393)	0.311 (0.298)	0.045 (0.332)
	P-value	0.090	**0.023**	**0.024**	**0.003**	0.853	0.208	0.858
$CD8^+$ T cells	WT	-0.305 (0.165)	-0.454 (0.225)	-0.605 (0.187)	-0.511 (0.228)	0.357 (0.433)	-0.264 (0.262)	-0.103 (0.408)
	KO	0.305 (0.442)	0.454 (0.374)	0.605 (0.331)	0.511 (0.350)	-0.357 (0.160)	0.264 (0.401)	0.103 (0.282)
	P-value	0.229	0.060	**0.008**	**0.030**	0.156	0.292	0.684

Table S8. Z-scores (mean ± SE) of phosphorylated protein levels in different immune cell populations isolated from MOG peptide primed *Atxn1*-null and wildtype mice (n=8) upon *in vitro* re-stimulation with MOG_{35-55} for 24 hours. Differences between groups were assessed by two-tailed Student's t-test.

Dataset S1 (separate file). Significant differentially expressed genes (DEGs) in *Atxn1* knockout and wildtype B cells.

Dataset S2 (separate file). GO analysis of the DEGs.

Dataset S3 (separate file). List of primers used in qRT-PCR validation experiments.